ATMOSPHERIC ENVIRONMENT: X 22 (2024) 100255

Contents lists available at ScienceDirect

Atmospheric Environment: X

journal homepage: www.journals.elsevier.com/atmospheric-environment-x

Long-term meteorology-adjusted and unadjusted trends of $PM_{2.5}$ using the AirGAM model over Delhi, 2007–2022

Chetna [a], Surendra K. Dhaka [b,*], Sam-Erik Walker [c], Vikas Rawat [a,d], Narendra Singh [d]

[a] Department of Physics and Astrophysics, University of Delhi, Delhi, India
[b] Radio and Atmospheric Physics Lab, Rajdhani College, University of Delhi, Delhi, India
[c] The Climate and Environmental Research Institute NILU, Kjeller, Norway
[d] Aryabhatta Research Institute of Observational Sciences, Manora Peak, Nainital, India

ARTICLE INFO

Keywords:
GAM
Particulate matter
Meteorology
Meteorology-adjusted trend

ABSTRACT

This study investigates the impact of meteorological variations on the long-term patterns of $PM_{2.5}$ in Delhi from 2007 to 2022 using the AirGAM 2022r1 model. Generalized Additive Modeling was employed to analyze meteorology-adjusted (removing the influence of inter-annual variations in meteorology) and unadjusted trends (trends without considering meteorology) while addressing auto-correlation. $PM_{2.5}$ levels showed a modest decline of 14 μg m^{-3} unadjusted and 18 μg m^{-3} meteorology-adjusted over the study period. Meteorological conditions and time factors significantly influenced trends. Temperature, wind speed, wind direction, humidity, boundary layer height, medium-height cloud cover, precipitation, and time variables including day-of-week, day-of-year, and overall time, were used as GAM model inputs. The model accounted for 55% of $PM_{2.5}$ variability (adjusted R-squared = 0.55). Day-of-week and medium-height cloud cover were non-significant, while other covariates were significant ($p < 0.05$), except for precipitation ($p < 0.1$). Wind speed (F-value: 98) showed the strongest correlation, followed by day-of-year (61), years (41.8), planetary boundary layer height (13.7), and temperature (13). Meteorological parameters exhibited significant long-term trends, except for temperature. Inter-annual meteorological variations minimally affected $PM_{2.5}$ trends. The model had a Pearson correlation of 0.72 with observed $PM_{2.5}$, underestimating episodic peaks due to long-range transport. Partial dependencies revealed a non-linear $PM_{2.5}$ relationship with meteorology. Break-point detection identified two potential breakpoints in $PM_{2.5}$ time series. The first, on October 1, 2010, saw a significant increase from 103.4 to 162.6 μg m^{-3}, potentially due to long-range transport. Comparing meteorology-adjusted and unadjusted trends can aid policymakers in understanding pollution change causes.

1. Introduction

Delhi, one of the world's megacities, has been plagued with severe particulate pollution for decades. It is earning notoriety as a pollution hotspot primarily due to the critical concentration level of $PM_{2.5}$ (Worldatlas, 2018). $PM_{2.5}$, a fine particulate matter with a diameter of 2.5 μm or less, poses a multifaceted threat to human health (Lin et al., 2018; Ma et al., 2018), climate (Liao et al., 2015), ecosystems, visibility (Fu et al., 2016), and overall air quality (Fuzzi et al., 2015). The chemical composition of particulate matter (PM) includes organic carbon (OC), elemental carbon (EC), and water-soluble inorganic ionic components (WSIC: sulfate, nitrate, chlorine, and ammonium). Over Delhi, the major sources of PM are the transportation sector, industries, dust and construction activities, and secondary aerosols. According to the Ministry of Earth Science (MoES) 2018 report The Automotive Research Association of India and The Energy and Resources Institute, (2018) on the new emission inventory, transport had the maximum contribution to the city's $PM_{2.5}$ (41%), followed by re-suspended dust (21.5%), industries (18.6%), and the rest (11%). The rest include municipal solid waste (MSW) plants, MSW open burning, crematoriums, the aviation sector, brick kilns, etc. Nagpure et al. (2015) reported that open MSW burning contributes 5–11% to Delhi's total $PM_{2.5}$ mass concentration. For $PM_{2.5}$, Jain et al. (2021) reported biomass burning combined with fossil fuel combustion (29%), secondary aerosol (26%), soil dust combined with sodium and magnesium salt (21%), vehicular emissions (18%), and industrial emissions (6%) as the major sources

* Corresponding author.
E-mail address: skdhaka@rajdhani.du.ac.in (S.K. Dhaka).

https://doi.org/10.1016/j.aeaoa.2024.100255
Received 30 September 2023; Received in revised form 21 February 2024; Accepted 26 March 2024
Available online 30 March 2024

over Delhi whereas for PM_{10}, major sources are soil dust combined with sodium and magnesium salt (29%), vehicular emissions (24%), secondary aerosol (20%), biomass burning combined with fossil fuel combustion (19%), and industrial emissions (7%). Vehicular emissions, followed by biomass burning are the dominant contributors of carbonaceous aerosols. A study by Latha et al. (2022) showed that secondary aerosols contribute 15–24% to the total $PM_{2.5}$. Biomass burning, vehicular emissions, crustal dust, and secondary aerosols are the major contributors to $PM_{2.5}$ levels. Water soluble ions like sulfate, nitrate, ammonium, and chloride contributed up to 50% of the total $PM_{2.5}$. A high correlation was observed between nitrate and sulfate ions indicating their common emission source. Jain et al. (2020) reported that secondary inorganic aerosols account for 27% of $PM_{2.5}$ concentrations and 21% of PM_{10} concentrations. The contribution of secondary sulfate is higher during summer and secondary nitrate is higher during winter. Traffic emissions are one of the major sources of PM_{10} pollution and biomass burning is for $PM_{2.5}$.

In addition to emissions from primary and secondary sources, meteorological parameters are also significant driving factors in determining the concentration at all time scales by governing its dispersion, transport, chemical transformations, dilution, and photochemical reactions within the atmosphere (Jing et al., 2020; Rawat et al., 2023; Tella et al., 2021). These meteorological factors also underpin chemical reactions that impact the concentration of secondary aerosols and ozone (Lu et al., 2019; Zhang et al., 2015). The interplay between meteorological conditions and baseline pollution was vividly demonstrated during the COVID-19 pandemic, where Dhaka et al. (2020) illuminated how various meteorological factors impact the concentration of fine particulate matter concentrations.

Long-term air quality trend analysis assumes paramount significance for the scientific community and policymakers and is a critical tool for discerning the underlying factors contributing to variations in pollutant concentrations. These fluctuations may stem from alterations in emission patterns, often attributable to policy interventions or meteorological influences. To isolate these two effects and quantify the efficacy of pollution mitigation strategies, it is imperative to remove the influence of temporal trends and meteorological variations within the time series of pollutant concentration. Conventional trend estimation techniques, such as the non-parametric Mann-Kendall test (Kendall, 1975; Mann, 1945) and the Theil-Sen slope estimator, are robust standard trend estimation techniques that can be employed to study trends in pollutant concentration. However, they cannot inherently capture the evolving and intricate dynamics of meteorological variables over time, which can wield considerable influence over long-term trends in pollutant concentration.

The non-linear and complex interactions between pollutants and meteorology cannot be fully described by linear models. Such interactions can be better addressed by advanced statistical methods like black-box machine learning models, regression trees, artificial neural networks, random forests, and generalized additive models (GAM). Although Machine-learning algorithms and artificial neural networks have high predictive power, they are complex and challenging to interpret (Stiglic et al., 2020). Grange et al. (2018) used a meteorological normalization technique based on a random forest machine-learning algorithm to study the PM_{10} trends in Switzerland from 1997 to 2016. Using the same technique, Grange and Carslaw (2019) studied the effect of air quality interventions in London. GAM modelling has been extensively used to study the complex and non-linear relationship between particulate matter (PM) and meteorology (Enayati Ahangar et al., 2021; Gao et al., 2023; Pearce et al., 2011). Solberg et al. (2021a) used GAM to study trends of air pollutants at the national level from 2005 to 2019 for European countries. Solberg et al. (2021b) also used GAM to study the impact of COVID-19 measures on NO_2 in Europe in 2020. In both of these studies, the recent air quality trend and prediction model AirGAM (Walker et al., 2023) was employed.

In the present study, AirGAM 2022r1 (Walker et al., 2023) was utilized to investigate the meteorological influence on long-term trends in $PM_{2.5}$ over Delhi during 2007–2022. The current study aims to analyze the meteorology-adjusted and unadjusted trends in $PM_{2.5}$ over Delhi and predict its concentrations using daily averages meteorological parameters as inputs. The meteorology-adjusted trends highlight the changes in pollutant concentration due to changes in emissions only, whereas unadjusted trends show the actual changes observed in the ambient $PM_{2.5}$ concentration, considering changes in emissions, meteorological conditions, or both. This comparative analysis between the meteorology-adjusted and unadjusted trends can be used in determining whether the observed changes in ambient pollutant levels are influenced by meteorological factors or the outcome of air pollution control measures.

Furthermore, our study employs break-point and break-segment detection techniques to identify significant transitions in the $PM_{2.5}$ time series over the 2007 to 2022 period. These breakpoints mark pivotal moments when notable changes in $PM_{2.5}$ concentrations occurred. By understanding these temporal shifts, we aim to deepen our comprehension of the intricate interplay between $PM_{2.5}$ and meteorological factors using the HYSPLIT backward air mass trajectory model. This knowledge is instrumental for refining our capacity to forecast air quality accurately and predict pollution events under varying meteorological conditions. Furthermore, our research builds upon prior work (Chetna et al., 2022), which synthesized insights from previous studies on Delhi's particle pollution trends. Together, this body of research contributes to a comprehensive perspective on the ever-evolving air quality landscape in Delhi, India, thereby facilitating informed decision-making and policy formulation to address air quality challenges effectively.

2. Materials and methods

2.1. Study area and its meteorology

Mega city Delhi is located (28.7° N, 77.1°E) in the Northern plains of India. It occupies an area of 1483 km^2, has 18 million inhabitants (https://www.census2011.co.in/census/state/delhi.html), and is situated at an elevation of 216 m above sea level. The map in Fig. 1 shows air quality monitoring stations and location of the city of Delhi, India. Due to the absence of any nearby large water bodies, the landlocked city experiences a semi-arid continental climate with significant variations in meteorological conditions, such as dry summers (relative humidity (RH): 48 ± 14%) with maximum temperature at 39 °C, moderate temperature with high humidity (71 ± 15% RH) in monsoon, moderate temperature (20 ± 5 °C) and relative humidity (67 ± 10%) in post-monsoon, and low temperatures up to 7 °C in winters. The supporting information Table S1 provides a season-wise statistical summary of $PM_{2.5}$ and all meteorological parameters from 2007 to 2022, classified into four major seasons: winter (January-February), summer (March-May), monsoon (June-September), and post-monsoon (October-December) according to IMD classification (IMD, 2015).

2.2. Data sources

Trend analysis was conducted on the daily average data set, obtained from various sources, including Central Pollution Control Board (CPCB), Delhi Pollution Control Committee (DPCC), and Indian Meteorological Department (IMD) and the U.S. Embassy and Consulates. The surface measurements of ambient daily $PM_{2.5}$ were obtained through the CPCB's online official portal (https://app.cpcbccr.com/ccr/#/caaqm–dashboard–all/caaqm–landing). The U.S. Embassy and Consulates also record the hourly average mass concentrations of $PM_{2.5}$ and have been available since 2013 from the Airnow website (https://www.airnow.gov/). $PM_{2.5}$ is measured using BAM-1022 by Met One Instruments Inc., based on the beta attenuation principle. The details of the instrument can be found in the manual (MetOne, 2020). The aerosol-loaded air sample is

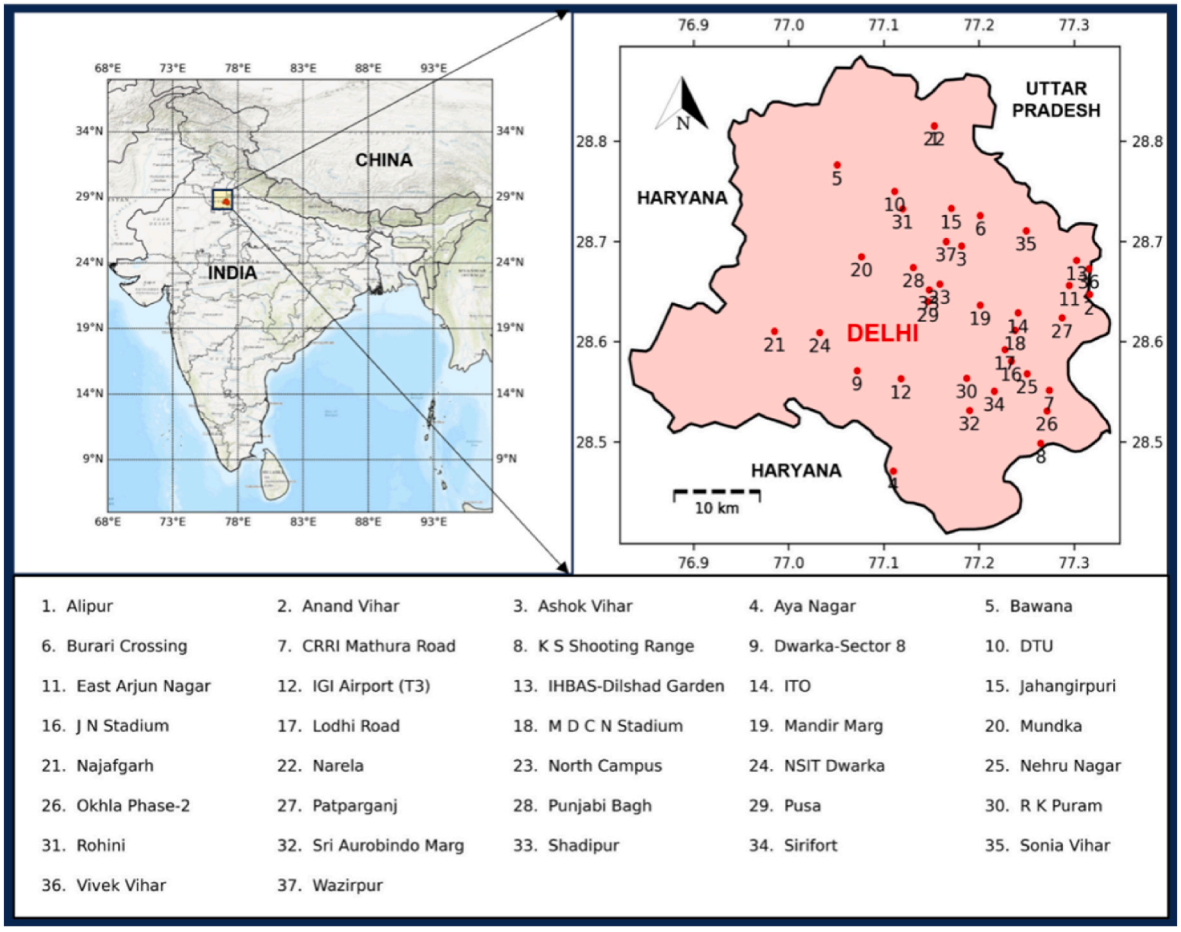

Fig. 1. Map of the study area depicting the location of Delhi in India and the locations of all 37 air quality monitoring stations situated in different zones of the city. The city is surrounded by Uttar Pradesh on its eastern side and Haryana on its western and south-western sides.

exposed to high-speed beta rays emitted from the C-14 source. The mass concentration of $PM_{2.5}$ is measured by observing the attenuation in beta particles. CPCB follows accepted international protocols and standard operating procedures (SoPs) to disseminate air quality and meteorological data for research purposes. The calibration and maintenance of the instruments are accomplished according to the guidelines and regulations of the U.S. Environmental Protection Agency (U.S. EPA) (2023). Details of the quality assurance and quality control (QA/QC) procedures are discussed in CPCB (2012) and on the CPCB website https://cpcb.nic.in/quality–assurance–quality–control/. Due to incomplete data from 2007 to 2022, it was impossible to conduct a trend analysis for each station individually. Therefore, we collected data from 37 monitoring stations across the city and calculated the average of all the station data to create a complete dataset representing the entire city.

The hourly average gridded meteorological data from the European Center for Medium-Range Weather Forecast (ECMWF) ERA5 reanalysis (Hersbach et al., 2020) was downloaded through the open-source Climate Data Store website https://cds.climate.copernicus.eu/. The dataset has a resolution of 0.25° × 0.25°, derived from the "ERA5 hourly data on single levels from 1940 to present" (https://doi.org/10.24381/cds.adbb2d47) in the NetCDF format. We used Python's 'xarray' module to focus on Delhi, within the coordinates of 28.40–28.88 °N and 76.84–77.34 °E, then transformed hourly data into daily, monthly, and yearly datasets. We acquired hourly mean data of temperature at 2 m, relative humidity at 2 m, wind speed and wind direction at 10 m, planetary boundary layer height, medium-height cloud cover and precipitation.

Our study used ERA5 data because meteorological data for all parameters from 2007 to 2022 was unavailable at any Delhi ground station. However, ERA5 data correlates well, Fig. S1 in the supplement, with ground meteorological data (Indira Gandhi International Airport, IGI station) and is used in various scientific studies. T. Singh et al. (2021) has shown that the ERA5 reanalysis data set can reasonably capture the spatial pattern of rainfall climatology over the Indian sub-continent during the study period of 1999–2018. Similarly, Vishal and Rani, 2022) shows near-surface (2m) air temperature estimates from Indian Monsoon Data Assimilation and Analysis (IMDAA) regional reanalysis estimates are highly correlated with ERA5 during 2000–2018 for 14 different stations selected over India.

2.3. GAM statistical modeling

The AirGAM model was implemented using the R programming language and software (R Core Team, 2022) with the "mgcv" (Wood, 2017), "openair" (Carslaw and Ropkins, 2012), and "sandwich" (Zeileis, 2022) packages. Due to the flexibility of smooth functions, the GAM model (Hastie and Tibshirani, 1990, 2017; Wood, 2017) is a straightforward and efficient tool to capture the intricate non-linear relationship between the local meteorological parameters and pollutant concentrations. The general equation of a GAM model is

$$g(\mu_i) = \beta_o + \beta_1(x_{1i}) + \beta_2(x_{2i}) + \ldots + \beta_n(x_{ni}) + \varepsilon \quad (1)$$

where $\mu_i = E(Y_i)$; subscript i is the day of the year, Y_i is the response variable (daily average concentration of $PM_{2.5}$); g is a link function; β_o is a constant (the intercept); β_1, β_2, …., β_n are the non-parametric smooth functions of the covariates; x_1, x_2, …., x_n are covariates; n is the number

of covariates; ε is the error term containing the residuals. Input meteorological data set consists of air temperature at 2 m in °C (x_1), wind speed in m s^{-1} (x_2), wind direction in degrees (x_3), relative humidity in % (x_4), planetary boundary layer height in m (x_5), medium-height cloud cover in % (x_6), daily total precipitation in mm day^{-1} (x_7). To account for temporal trends, including daily and seasonal variations, weekday and weekend effects on the emissions, the time covariates viz. day-of-week (x_8), day-of-year (x_9), and overall time (x_{10}) were also given as a GAM input. Overall time (x_{10}) represents the trend term in pollutants; it is continuous time in a fraction of years with 0.0 = 1 January 2007 at the start of the period. For $PM_{2.5}$, a log-transformation is used as the link function in Eq. (1) so the mathematical equation for the GAM model for $PM_{2.5}$ is given as

$$\log(E(Y_i)) = \beta_o + \beta_1(x_{1i}) + \beta_2(x_{2i}) + \ldots + \beta_9\,(x_{9i}) + \beta_{10}\,(x_{10i}) \quad (2)$$

with x_1, x_2, …., x_{10} the meteorological and time variables. The smooth function $\beta_{10}(t)$ corresponding to overall time (x_{10}) in Eq. (2) represents the meteorology-adjusted trend. The daily average concentration of $PM_{2.5}$ was used as a dependent or response variable (Y), and meteorological and time covariates were used as independent variables. The response variable has a definite probability distribution, and its expected value is μ. The link function, g(μ), links the expected value of Y to the covariates. The $PM_{2.5}$ distribution is not Gaussian but typically highly skewed towards the right, so a gamma distribution and a log link function, g(μ) = log(μ), were chosen for such a right-skewed distribution (Wood, 2017) to make the residuals closer to a normal distribution. Cubic regression splines were used as smooth functions for all covariates to investigate the association between $PM_{2.5}$ and meteorology. For wind direction, cyclic cubic splines were used. The model coefficients and smoothing parameters were estimated using restricted maximum likelihood, REML, as the fitting method. The standard and default ten basis functions (k = 10) were used for all meteorological and 'day-of-year' covariates, whereas k = 9 was used for the 'years' time covariate. The standard and default ten basis functions (k = 10) were used for all meteorological and 'day-of-year' and 'years' covariates. The 'day--of-week' covariate takes values from 1 to 7, corresponding to Monday to Sunday, but is handled as a continuous variable using seven basis functions. The present method assumes that an additive combination of the local meteorology and the time variables without any interactions between them are sufficient to estimate the daily mean pollutant concentration. However, due to the very different nature of the meteorological seasons in Delhi, we employ a separate set of smooth functions for the meteorological variables for each season. For the time variables, including for the trend, a single smooth function covering all four seasons are used. GAM performance is evaluated by standard statistical metrics like R^2, root mean square error (RMSE), and mean bias (MB). Unadjusted trends are calculated by removing meteorological variables from GAM and keeping only the time covariates. It represents the actual observed trends in pollutant concentrations in ambient air. An AR (1) auto-regressive time series model of order one is included to handle autocorrelation in the model residuals. The model's predictive power is evaluated using the out-of-year cross-validation method for the entire study period (2007–2022).

The GAM model in AirGAM is a nonlinear regression model using observed concentrations ($PM_{2.5}$) as response variables and daily average data of local meteorology and other time data as input covariates. The model estimates a smooth function of each covariate from these data, representing the nonlinear relationship between the expected concentration value on each day and the corresponding meteorology and time data. The last covariate (β_{10} in Equation (2)) in the model represents the concentration trend term and is also estimated as a smooth function of total time (days) from the beginning of the analysis period. In this way, our model aims to discount the effect of any day-to-day time variations or trends in the meteorological data when estimating the concentration trend term, which may be considered a meteorology-adjusted trend over time. Thus, in our approach, there is no need to use a chemical transport model (CTM) or to hold the meteorology constant from the beginning of the analysis period. Unlike other methods, this model doesn't assume that the weather conditions stay constant throughout the analysis period. The model does not explicitly include emissions or background concentrations. Instead, it aims to indirectly estimate these trends by addressing the complex connections between local meteorology, time, and $PM_{2.5}$ concentrations.

3. Results and discussion

3.1. Overview of particle pollution in Delhi

From 2007 to 2022, the daily average mass concentration of $PM_{2.5}$ was 122 ± 82 μg m^{-3}, with values ranging between 21 and 754 μg m^{-3}. In accordance with Indian NAAQS, the permissible daily and annual average concentrations of $PM_{2.5}$ are 60 μg m^{-3} and 40 μg m^{-3}, respectively. Throughout the entire study period, the daily average $PM_{2.5}$ concentration exceeded the critical levels set by the Indian national standards (CPCB, 2009). The symbol ± represents the standard deviation in $PM_{2.5}$ values as observed in our data from 2007 to 2022. Seasonally, the average mass concentration of $PM_{2.5}$ was 170 ± 75 μg m^{-3} in winter, 100 ± 46 μg m^{-3} in summer, 63 ± 39 μg m^{-3} in the monsoon season, and 188 ± 90 μg m^{-3} in the post-monsoon season. The highest concentration was observed during the post-monsoon season, followed by winter and summer, while the monsoon season had the lowest concentration. Table 1 presents the descriptive statistics of $PM_{2.5}$ and the meteorological data set during the study period.

The season-wise statistical summary of $PM_{2.5}$ and meteorological parameters during 2007–2022 over Delhi is given in supplement file Table S1.

Yang et al. (2018) reported a fluctuating trend in $PM_{2.5}$ over Delhi from 2014 to 2017 indicating variability in pollution levels during that period. Contrasting this, Sharma et al. (2018) observed non-significant increasing trends in organic carbon, elemental carbon, and PM_{10} ($y = 6.785x + 194.8$, $R^2 = 0.241$) during 2010–2017 over Delhi. Their findings underscore the complexity of pollutants' behavior in urban environments. Hammer et al. (2020) reported a rising trend in population-weighted mean geophysical $PM_{2.5}$ values over India at the rate of 1.13 ± 0.15 μg m^{-3} $year^{-1}$ from 1998 to 2018; 2.44 ± 0.44 μg m^{-3} $year^{-1}$ from 2005 to 2013 period and a declining trend at the rate of −0.54 ± 0.7 μg m^{-3} $year^{-1}$ during 2011–2018. Such fluctuations reveal the dynamic nature of pollution trends over time. V. Singh et al. (2021) analyzed data from the U.S. Embassy and Consulate to assess the annual trend in $PM_{2.5}$ for five Indian megacities from 2014 to 2019 and reported a decline in $PM_{2.5}$ at a rate of 4.19 ± 1.12 μg m^{-3} $year^{-1}$ for New Delhi, highlighting potential improvements in air quality management efforts, particularly notable in New Delhi. In contrast. D. Sharma and Mauzerall (2022) found no significant trend in $PM_{2.5}$ over Delhi observed during the 2015–2019 period using the U S Embassy and Consulate hourly data, suggesting a potential stabilization or plateauing of pollution levels during this period. Furthermore, recent findings by S. K. Sharma et al. (2022) during Jan 2012–April 2021 period revealed a non-significant decreasing trend ($R^2 = 0.18$) in annual $PM_{2.5}$ levels but a significant decreasing trend in elemental carbon (EC), organic carbon (OC), and total carbon (TC) over Delhi, indicating potential shifts in pollutant composition.

Collectively, these studies emphasize the multifaceted nature of air pollution trends in Delhi and India, highlighting the importance of continuous monitoring and targeted interventions to mitigate the adverse impacts of air pollution on public health and the environment.

3.2. Meteorology-adjusted and unadjusted trends

3.2.1. Generalized additive mixed model (GAMM) for $PM_{2.5}$

The raw auto-correlation and partial auto-correlation residuals plots

Table 1
Statistical summary for the daily mean measurements of $PM_{2.5}$, temperature (Temp, °C), wind speed (WS, m s^{-1}), wind direction (WD, °), relative humidity (RH, %), medium-height cloud cover (MCC, %), and planetary boundary layer height (PBLH, m).

(2007–2022)	$PM_{2.5}$ (μg m^{-3})	Temp (°C)	Wind speed (m s^{-1})	Wind direction (degree)	RH (%)	MCC (%)	PBLH (m)
Average	122	25	2	220	65	12	514
St. Dev	82	7	1	106	16	16	254
Median	102	27	2	279	68	6	444
Max	754	40	7	360	99	100	1483
Min	21	6	0	0	21	0	114

for a meteorology-adjusted model for $PM_{2.5}$ are depicted in the LHS panel of Fig. 2. Significant high auto-correlation was present in the model with lag-1 value as the most significant. Auto-correlation function (ACF) values slowly decayed with an increasing time lag. To handle this, we used a generalized additive mixed model (GAMM) using the 'gamm' routine of the 'mgcv' R package (S. Wood, 2023; S. N. Wood, 2017) available as part of the AirGAM 2022r1 model system. This routine includes an auto-regressive order-1 AR(1) model with a one-day time lag for model residuals. The RHS panel of Fig. 2 clearly shows that the GAMM model resulted in non-significant correlations; thus, auto-correlation was handled efficiently. Ito et al. (2007) reported that $PM_{2.5}$ levels on a given day are influenced by the weather conditions of the preceding day. In the present work, the entire analysis for the complete year was done using the GAMM model. R-sq. (adj) was found to be 0.55, thus approximately 55% of the variations in the $PM_{2.5}$ concentration can be explained by the model covariates. Except for medium-height cloud cover and day-of-week, all meteorological and time variables were found to be statistically significant (p-value <0.05) for the converged $PM_{2.5}$ AR(1) GAM model. It is essential to mention that precipitation is significant only at a 10% significance level. The significance of each term in a GAM summary is evaluated by the F-value for each smooth function, which measures how well each term explains the variations in the response variable. Based on the F-value, wind speed (F-value: 98) was the strongest covariate, followed by day-of-year (61). Among the meteorological variables, wind speed (F-value: 98), planetary boundary layer height (13.7), and temperature (13.0) were dominant. Except for wind speed, all the predictors were non-linearly associated with $PM_{2.5}$ with an empirical degree of freedom (edf) value > 1. Section 3.3.4 contains a closer description of these non-linear relations as estimated by the model.

The meteorology-adjusted and unadjusted trends in $PM_{2.5}$ during the study period are shown in Fig. 3. Clear seasonal variations were observed in $PM_{2.5}$ during the 16-year-long data set. The minimum observed monthly average $PM_{2.5}$ concentration during the study period was 32 μg m^{-3} in August 2020, and the maximum was 294 μg m^{-3} in November 2016. Both meteorology-adjusted and unadjusted trends showed overall non-linear declining trends with fluctuations. Initially, the meteorology-adjusted concentration decreased from 2007 (115 μg m^{-3}) to mid of 2008 (113 μg m^{-3}). Afterwards, it continuously increased up to the beginning of 2013 (155 μg m^{-3}). A significant decline was observed from 2013 until 2022 (97 μg m^{-3}). Overall, the trend declined from 115 μg m^{-3} in 2007 to 97 μg m^{-3} in 2022, a decrease of only 18 μg m^{-3} during 2007–2022. It is clear from the plot that the meteorology-adjusted and unadjusted trends are pretty close to each other after 2015.

Since 2015, the meteorology-adjusted and unadjusted trends have nearly converged, indicating minimal impact from inter-annual meteorological variations on $PM_{2.5}$ trends. Theil-Sen trends of meteorological parameters from 2015 to 2022 is shown in Fig. S5. It reveals a notable positive trend in relative humidity (0.31 % $year^{-1}$; 95% confidence interval [0.03, 0.58], $p < 0.05$) and a declining trend in wind direction ($-8.47°$ $year^{-1}$; 95% CI [−10.44, −5.27], $p < 0.001$). However, no statistically significant trends were observed in other meteorological factors such as temperature, wind speed, planetary boundary layer height, and rainfall. Consequently, the marginal increase in relative humidity, changes in wind direction, and potential other factors appear to counterbalance each other's effects, resulting in nearly identical

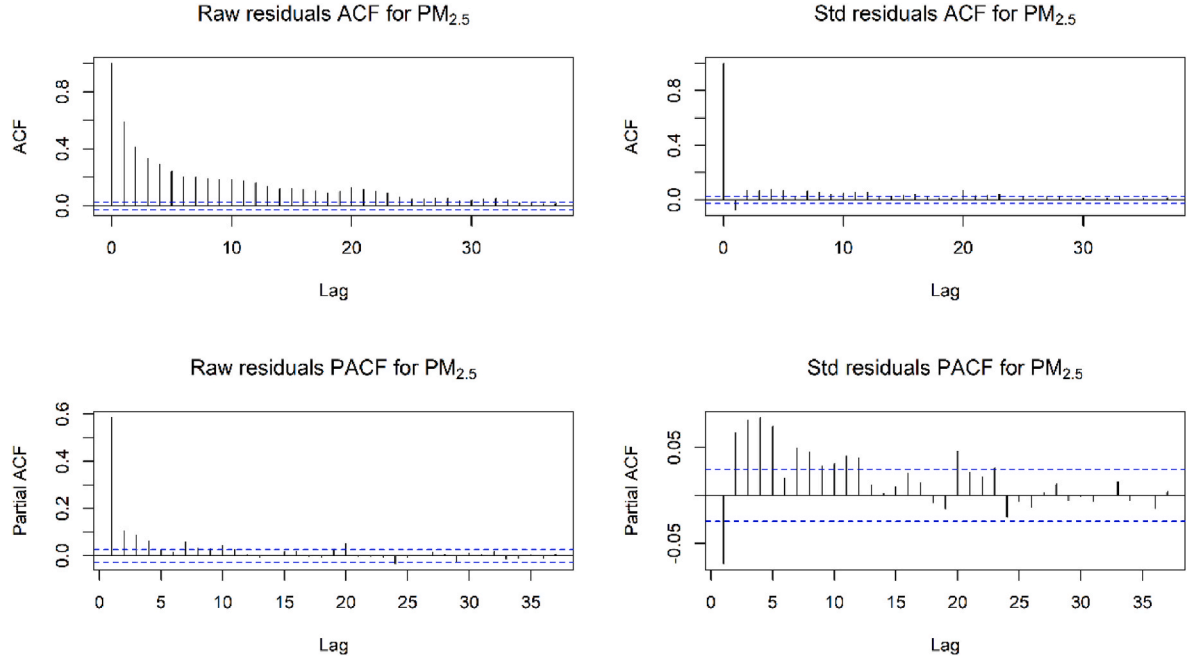

Fig. 2. LHS panel shows raw auto-correlation function (ACF), and partial auto-correlation function plots and the RHS panel shows GAMM standardised auto-correlation and partial auto-correlation plots for $PM_{2.5}$ for the meteorology-adjusted model error residuals at Delhi for 2007–2022.

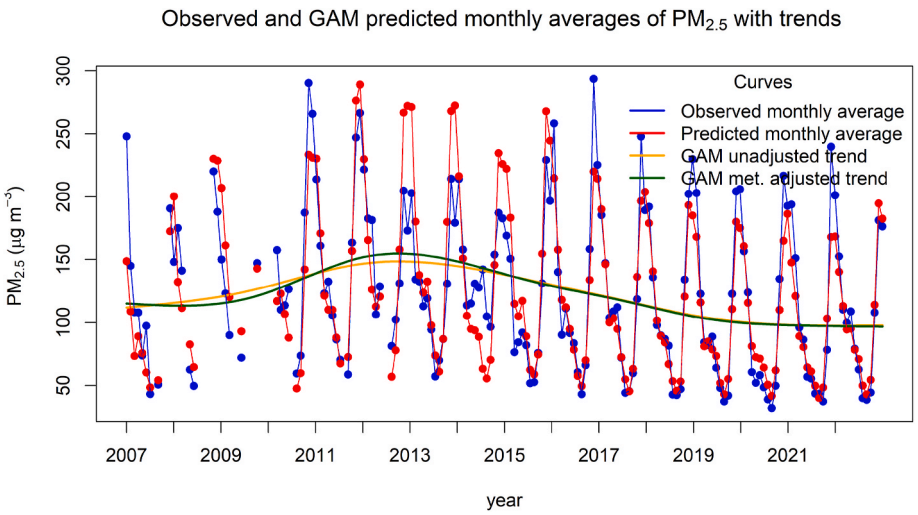

Fig. 3. Observed (blue curve) and predicted (red curve) monthly average $PM_{2.5}$ concentrations in Delhi during 2007–2022. The meteorology-adjusted and unadjusted smooth trend curves are shown in green and orange colors, respectively. (For interpretation of the references to colour in this figure legend, the reader is referred to the Web version of this article.)

meteorology-adjusted and unadjusted $PM_{2.5}$ trends since 2015.

The unadjusted component started rising from 2007 (112 μg m^{-3}) till the end of 2012 (149 μg m^{-3}); afterwards, it continuously showed a downtrend up to the end of 2022 (98 μg m^{-3}). Overall, the unadjusted trend declined from 112 μg m^{-3} in 2007 to 98 μg m^{-3} in 2022, a decrease of only 14 μg m^{-3} during 2007–2022. Overall, the inter-annual meteorological variability has not considerably affected the long-term trends in $PM_{2.5}$ over Delhi during 2007–2022. In Fig. 3, blue and red circles show the observed and GAM-predicted monthly average $PM_{2.5}$ concentrations, respectively. The concentrations are either underestimated or overestimated probably because the $PM_{2.5}$ peaks are associated with the long-range transport of pollution, which is not

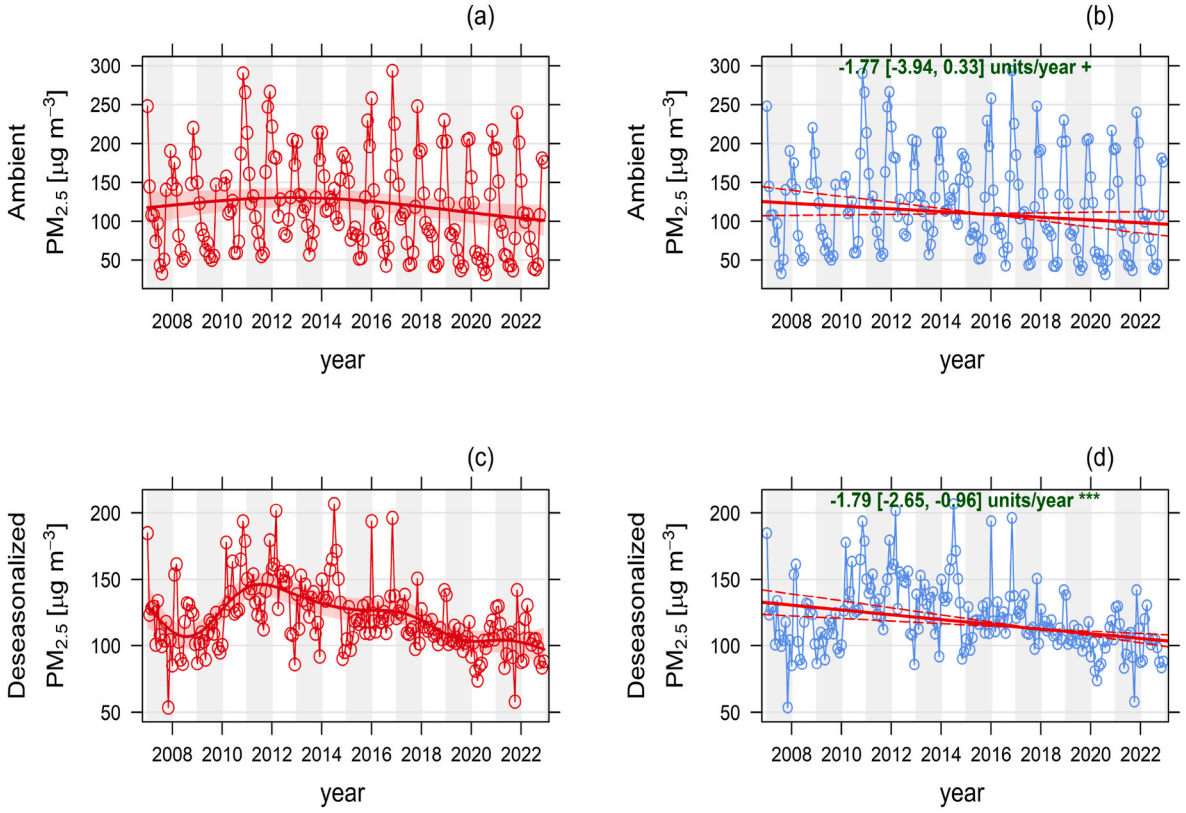

Fig. 4. Panel **a)** displays a smooth-trend plot of ambient $PM_{2.5}$, while panel **c)** represents the de-seasonalized $PM_{2.5}$. Panel **b)** shows the inter-annual Theil-Sen linear trends in ambient $PM_{2.5}$, while panel **d)** represents the same for de-seasonalized $PM_{2.5}$. The monthly mean concentration is shown by blue circles. A trend estimate is represented by a red line, while a dashed red line illustrates the 95% confidence interval (CI) for the trend, calculated using resampling methods. The overall trend is displayed in the top-left corner, expressed in μg m^{-3} $year^{-1}$, with the corresponding 95% CI for the slope or trend indicated in square brackets. Significance levels are denoted by symbols: *** ($p < 0.001$), ** ($p < 0.01$), * ($p < 0.05$), and + ($p < 0.1$). (For interpretation of the references to colour in this figure legend, the reader is referred to the Web version of this article.)

correlated with the local meteorology of the region and hence cannot be captured by the GAM. A concurvity analysis was also performed, and we found that all the covariates were reasonably independent. Fig. S2 in the supplement illustrates the monthly median $PM_{2.5}$ values at Delhi from 2007 to 2022, represented by blue and red colors for the observed and GAM predicted values, respectively. As for the mean, the figure reveals a lack of data coverage prior to 2011, and it is evident that the GAM model occasionally underestimates or overestimates the $PM_{2.5}$ values. Our study incorporates data from the COVID-19 period. However, Theil-Sen and GAM smooth-trend analyses (not shown) demonstrated a downward trend in $PM_{2.5}$ levels even with excluding the COVID-19 period, but with a reduced magnitude. Furthermore, using GAM as a prediction tool, the observed and GAM-predicted PM2.5 concentration are in good agreement for lockdown years 2020 and 2021. This decline in particular pollution can be attributed to the government's various initiatives and mitigation measures taken to tackle air pollution in Delhi-NCR, as detailed in Table S2 of the supplement.

3.2.2. *Theil-Sen and GAM smooth-trend analysis*

The openair R package (Carslaw and Ropkins, 2012) was used to analyze trends in $PM_{2.5}$ levels over Delhi from 2007 to 2022. The Theil-Sen function (Sen, 1968; Theil, 1950) implements Theil-Sen regression analysis and provides the non-parametric measurements of trends (Ropkins and Carslaw, 2012). Chetna et al. (2022) used it to estimate the trends in $PM_{2.5}$ over Delhi during 2007–2021.

The Theil-Sen linear trend is calculated using monthly mean concentrations, denoted in Fig. 4 by the blue circles. The solid red line represents the trend estimate, and the dashed red line indicates the 95% confidence interval (CI) of the trend obtained through bootstrap resampling methods. The overall trend for Delhi from 2007 to 2022 is displayed at the top-left corner, indicating a decrease of -1.77 μg m^{-3} $year^{-1}$ for ambient $PM_{2.5}$ and -1.79 μg m^{-3} $year^{-1}$ for de-seasonalized $PM_{2.5}$. The square bracket denotes the 95% confidence interval (CI) of the trend. The significance levels of the trend are denoted by ***, **, *, and +, indicating significance at the 0.001, 0.01, 0.05, and 0.1 levels, respectively (see Fig. 5).

The smoothTrend function in openair R package gives the smooth trend line using the non-parametric generalized additive modelling technique. Fig. 4a shows that the overall trend in ambient $PM_{2.5}$ is non-linear. A rise in ambient $PM_{2.5}$ levels was observed from 2007 to 2012. Afterwards, a decreasing trend in $PM_{2.5}$ levels despite rising human and vehicle populations, small-scale factories and industries, and substantial construction activities in the Delhi-NCR region. Fig. 4c shows the smooth-trend plot in the de-seasonalized $PM_{2.5}$ time series. Between 2007 and 2008, there was an initial decrease in $PM_{2.5}$ levels. However, from 2008 to 2012, there was a continuous rise in $PM_{2.5}$ levels. Subsequently, a downtrend was observed from 2013 until 2022. A linear estimate using the Theil-Sen estimator showed a declining trend in both ambient (Fig. 4b) and de-seasonalized (Fig. 4d) $PM_{2.5}$ time series with an average decrease of -1.77 [95% CI: 3.94, 0.33] μg m^{-3} $year^{-1}$ at $p < 0.1$

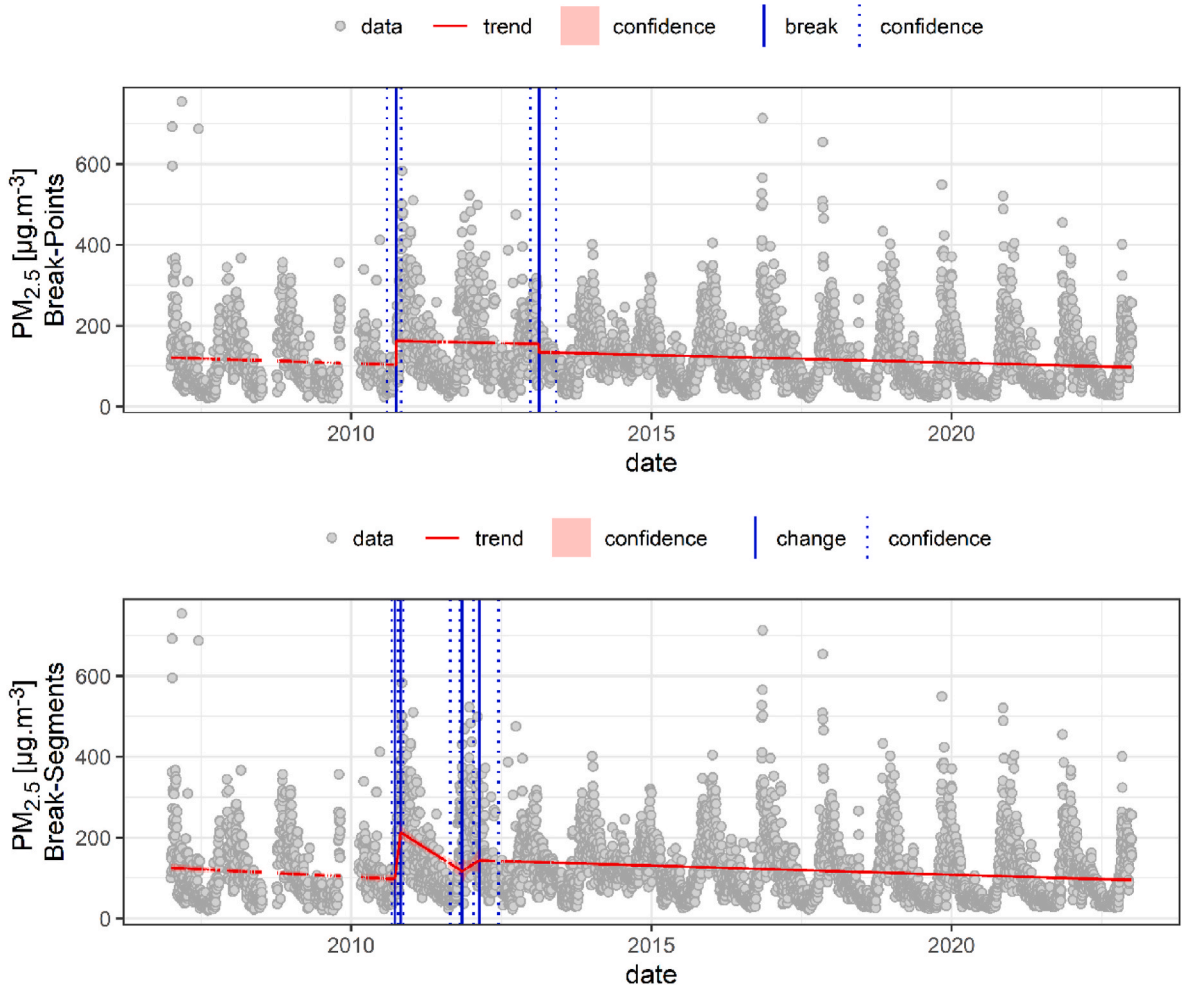

Fig. 5. Break-point detection and change-segment analysis of ambient $PM_{2.5}$ time-series at one day resolution for Delhi during 2007–2022. It is created using 'quantBreakPoints' and 'quantBreakSegments' functions of AQEval R package. The solid blue line represents the statistically significant break point in the time series and dotted blue line shows the associated 95% confidence intervals determined using the 'strucchange' methods. (For interpretation of the references to colour in this figure legend, the reader is referred to the Web version of this article.)

and −1.79 [95% CI: 2.65, −0.96] μg m^{-3} $year^{-1}$ at $p < 0.001$ level of significance respectively. It indicates $PM_{2.5}$ approximately decreased by 29 μg m^{-3} during 2007–2022 over Delhi. It is essential to mention that with the de-seasonalization of the data, there is a minimal effect (1 μg m^{-3}) on the magnitude of the trend. However, the 95% confidence interval and significance level of the trend get improved drastically. Also, by employing the Theil-Sen regression technique, we derived an estimate of the linear trend across the complete study period. This method assumes a monotonically increasing or decreasing trend. However, leveraging a GAM model, we obtained a more refined estimate using non-linear regression techniques. Consequently, the linear trend estimate surpasses the GAM estimate due to the latter's ability to capture complex non-linear trends more effectively.

3.2.3. Standalone break-point/segment testing

The AQEval R package (Ropkins et al., 2023) has been used to identify and analyze the structural changes in the ambient pollutant time series. Ropkins et al. (2022) used this package to measure the impact of air quality related interventions in Leeds, UK.

The 'strucchange' R package of Zeileis and colleagues (Zeileis et al., 2002, 2003, 2008) describes robust statistical techniques to identify the structural changes in the time series.

The break-point detection methods identify the significant break-points in the time series by applying the rolling window approach. In this approach, the linear regression properties of the pollutant time series are tested. It is based on the hypothesis that a break-point exists if the surrounding data can be better explained by two discrete models rather than one general model. Multiple break-points can also be identified with a 95% confidence interval. The break-point testing was applied to the complete time series with a time window/test window of 15% (h = 0.15) of the length of the time series. In the rolling window approach, the size of the window determines the number of observations used in the analysis at each step. A potential structural change was identified, also known as a break-point (s) in the time series. Test statistics at a 0.05 significance level are calculated to check the statistical significance of each identified break-point. This method helps detect shifts in trends and patterns. The 'Muggeo method' (V. M. Muggeo, 2008; V. M. R. Muggeo, 2003, 2017, 2023) extends break-point methods to identify regions of likely change (break-segment), allowing for the detection of gradual changes in a time series. Ropkins & Tate (2021) have used break-point and break-segment methods to identify the impact of COVID-19 lockdown on air quality trends in UK. Break-point and break-segment methods were directly applied to the ambient measurements of $PM_{2.5}$. Break-point testing conducted on the ambient $PM_{2.5}$ time series in Delhi revealed the presence of two potential break points. The first break point occurred on October 1, 2010, with a 95% confidence range spanning from August 7, 2010, to November 2, 2010. The second break point was observed on February 15, 2013, within the confidence range of December 24, 2012, to May 29, 2013. The first break point, occurring on October 1, 2010, was associated with a significant increase in $PM_{2.5}$ levels from 103.4 to 162.6 μg m^{-3}, representing a rise of 59 μg m^{-3} or a 57% increase. To understand this spike, five-day back trajectories pathways are computed at every 6-h intervals using the Hybrid Single-Particle Lagrangian Integrated Trajectory (HYSPLIT) model. This computational effort spans from the 7th of August to the 2nd of November in the year 2010. The primary objective of this analysis is to find the distinct contributions of remote and regional sources of pollutants to the atmospheric composition of Delhi within the 95% confidence interval of the breakpoint event. To facilitate these investigations, an archive reanalysis dataset sourced from the National Centers for Environmental Predictions (NCEP) is employed within the HYSPLIT framework. This dataset is characterized by a spatial resolution of 2.5° and encompasses 17 discrete pressure levels.

Out of a total of 348 calculated trajectories over the given period, Total Spatial Variance (TSV) is calculated to combine close trajectories into five distinct clusters. Of particular significance are the trajectories denoted as red (23%) and magenta (7%), originating from the geographical location of Iran and Afghanistan. These trajectories are underscored by their propensity to transport pollutants over extended distances, thereby implicating them as substantial contributors to long-range pollutant influx and subsequent deposition within the Delhi region. In contrast, the remaining trajectories predominantly exhibit regional and local influences, contributing in excess of 65% to the observed air quality deterioration within the study domain of Delhi during the established investigation period. An additional salient observation pertains to the year 2010, during which the Commonwealth Games were prominently hosted within the Delhi region. The second break point, on February 15, 2013, was associated with a decrease in $PM_{2.5}$ levels from 155 to 135 μg m^{-3}, indicating a drop of 20 μg m^{-3} or a 13% reduction in $PM_{2.5}$ levels. Additionally, change-segment modeling analysis revealed five distinct periods of change (segments) in the $PM_{2.5}$ time series, as presented in Table S3 in the supplement. The model indicated a general decrease in $PM_{2.5}$ concentration from 2007 to 2010, amounting to approximately 22% over four years. This was followed by a rapid step increase between September 23, 2010, and October 29, 2010, with a staggering 116% rise within just 36 days. Subsequently, a significant reduction of 45% in $PM_{2.5}$ levels was observed from November 2010 to 2011. From November 2011 to February 2012 (spanning 106 days), $PM_{2.5}$ concentration experienced a 22% increase. Finally, over a prolonged period of 11 years (2012–2022), $PM_{2.5}$ levels dropped from 144 μg m^{-3} to 96 μg m^{-3}, indicating a decrease of 34% (see Fig. 6).

3.2.4. Partial dependencies of meteorological and time covariates with $PM_{2.5}$

Fig. 7 displays partial effects plots for all meteorological and time covariates of the $PM_{2.5}$ GAMM model for 2007–2022, elucidating the relationship between $PM_{2.5}$ and meteorological and time variables. Notably, all the plotted partial effects are between the log of $PM_{2.5}$ concentration and each covariate. The relationship between temperature and fine particles depends on the temperature range. Initially, as the

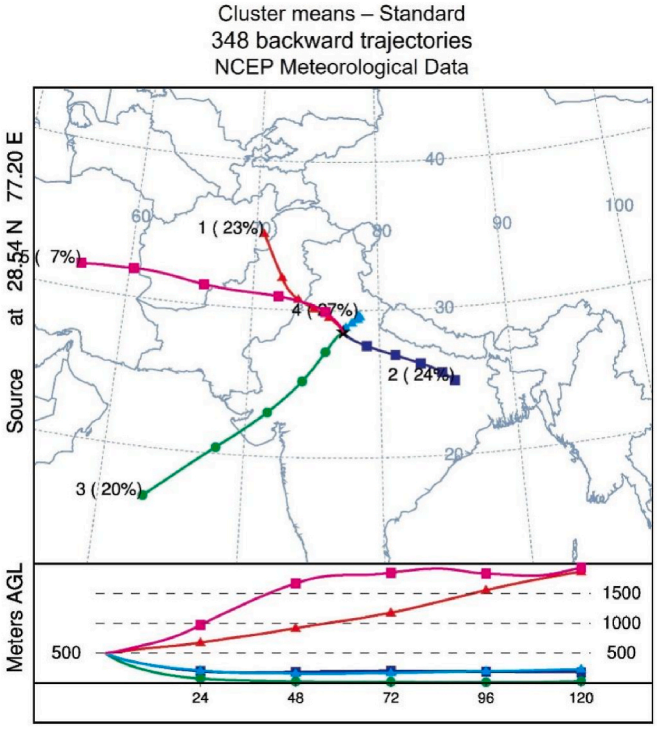

Fig. 6. Five days back-trajectory cluster analysis over Delhi starting at 500 m height above ground from August 7, 2010 to November 2, 2010.

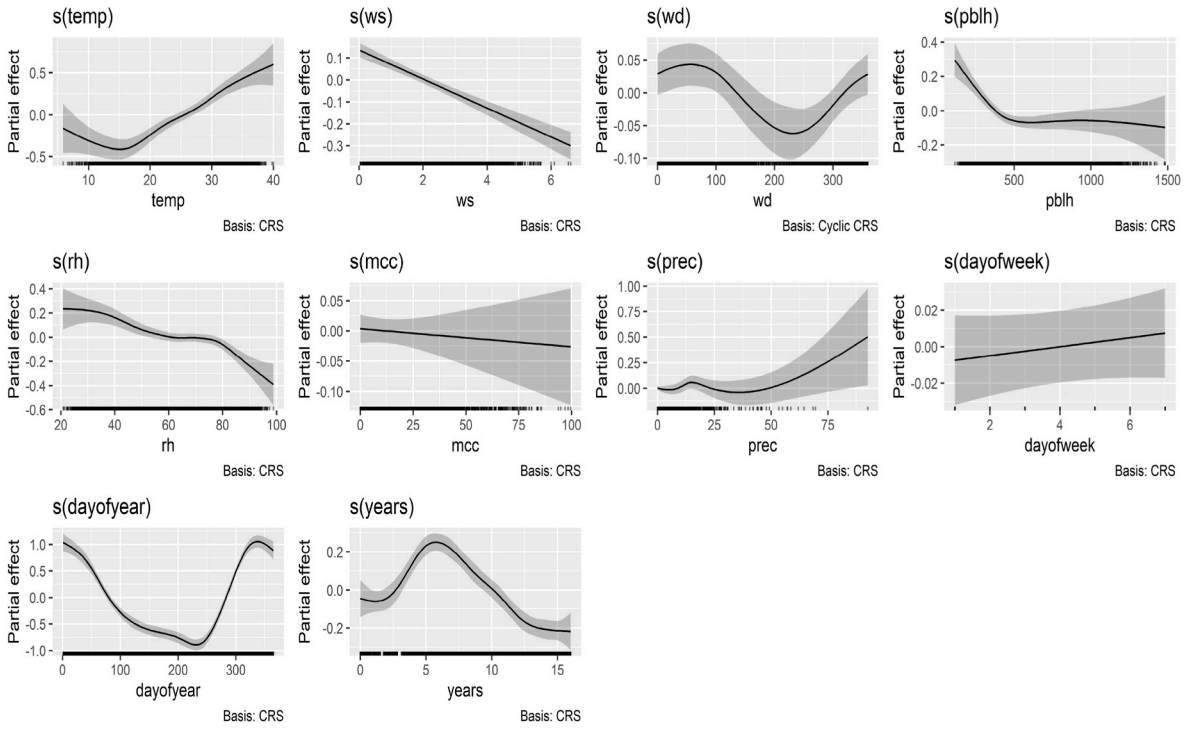

Fig. 7. Partial effects plots for the meteorological and time variables of AR (1) GAM model for $PM_{2.5}$ during 2007–2022. temp, ws, wd, pblh, rh, mcc, and prec represent temperature, wind speed, wind direction, planetary boundary layer height, relative humidity, medium-height cloud cover, and precipitation, respectively. 's()' represent the smooth function of the GAM model. CRS at the bottom of each subplot and cyclic CRS for wind direction show that cubic regression and cyclic cubic regression splines are used as smooth functions, respectively. The grey-shaded area represents the 95% confidence region for the curve. Notably, all the plotted partial effects are between the log of $PM_{2.5}$ concentration and each covariate.

temperature rises to 15 °C, $PM_{2.5}$ levels decrease. However, as the temperature rises from 15 °C to 40 °C, $PM_{2.5}$ shows a non-linear increase. Yang et al. (2016) state that an increase in temperature can improve air circulation, atmospheric turbulence, and thermal movements, which decrease the concentration of $PM_{2.5}$. After reaching 15 °C, we observe a positive association between $PM_{2.5}$ and temperature, which can be attributed to the formation of secondary particulate matter from photochemical reactions between the precursors. Whiteman et al. (2014) report that high temperatures and longer duration of sunlight promote photochemical reactions and the formation of secondary aerosols.

Wind speed is a crucial parameter that strongly affects fine particle concentrations (Fig. 7). As wind speed increases, $PM_{2.5}$ mass concentration decreases. Higher wind speeds disperse and dilute suspended fine particulates, resulting in lower concentrations near the ground. Moderate wind speeds dilute suspended PM (Wu and Zhang, 2019). Wang and Ogawa (2015) suggest a threshold wind speed beyond which the association between $PM_{2.5}$ and wind speed changes direction. We observe a peak for wind direction, specifically the north-westerly direction, while south-westerly winds are associated with low $PM_{2.5}$ levels.

As the *planetary boundary layer height (PBLH)* increases up to 500 m, there is a sharp decrease in $PM_{2.5}$. However, as PBLH rises above 500 m, we observe almost no change in $PM_{2.5}$ mass concentration. Luan et al. (2018) and Miao et al. (2018) find a non-linear negative correlation between $PM_{2.5}$ and PBLH. The relationship between PBLH and PM is not necessarily always significant and negative (Geiß et al., 2017). According to Su et al. (2018) the association between particulate matter and PBLH is influenced by numerous factors, such as season, topography, and meteorological conditions. Particularly noteworthy interactions occur during shallow PBLH, leading to elevated $PM_{2.5}$ levels. *Precipitation* is a significant variable, but only at a 10% level of significance. We observe a negative relationship between precipitation and $PM_{2.5}$. Precipitation has a scavenging effect on air pollution (Li et al., 2014).

A negative and non-linear relationship was observed between $PM_{2.5}$ and relative humidity (RH). This may be attributed to the absorption of atmospheric moisture by suspended particles leading to swollen and bulky particulate matter (PM), which cannot remain suspended in air and finally results in their dry deposition. Wang and Ogawa (2015) also observed a strong negative correlation between $PM_{2.5}$ and relative humidity. Fig. S6 in the supplement shows the correlation plot between $PM_{2.5}$ and all meteorological parameters.

Day of the week was not a statistically significant variable. However, $PM_{2.5}$ levels were strongly associated with the Julian day of the year (1–365/366). From January-March (1st–100th days), $PM_{2.5}$ showed an almost linear decrease in concentrations, but from April-June (100th–200th days), the decrease was tiny and non-linear. After the 250th day (September), $PM_{2.5}$ concentration increased linearly, reaching its peak in November, with a slight decrease in December. The years covariate shows that the trend of $PM_{2.5}$ fluctuates, but there is an overall weak downtrend over the 16-year study period.

3.3. Performance of the GAM model

Fig. 8 depicts the model evaluation plots for the meteorology-adjusted model of $PM_{2.5}$ for the period 2007–2022. The upper-left plot displays the quantiles of the model residuals against the theoretical quantiles, assuming a Gaussian distribution for the residuals. Black data points represent the $PM_{2.5}$ residuals, and they deviate from the straight line representing a good model fit only at the upper tail portion. However, it is worth noting that the $PM_{2.5}$ residuals also deviates, but only slightly so, at the lower extremes. The remaining subplots of the model evaluation plots for $PM_{2.5}$ closely resemble the ideal plots.

Fig. 9a shows the conditional quantile plot for the $PM_{2.5}$ GAM model for the 2007–2022 cross-validation period. The graph shows the light and dark yellow shades, which represent the 10/90th and 25/75th

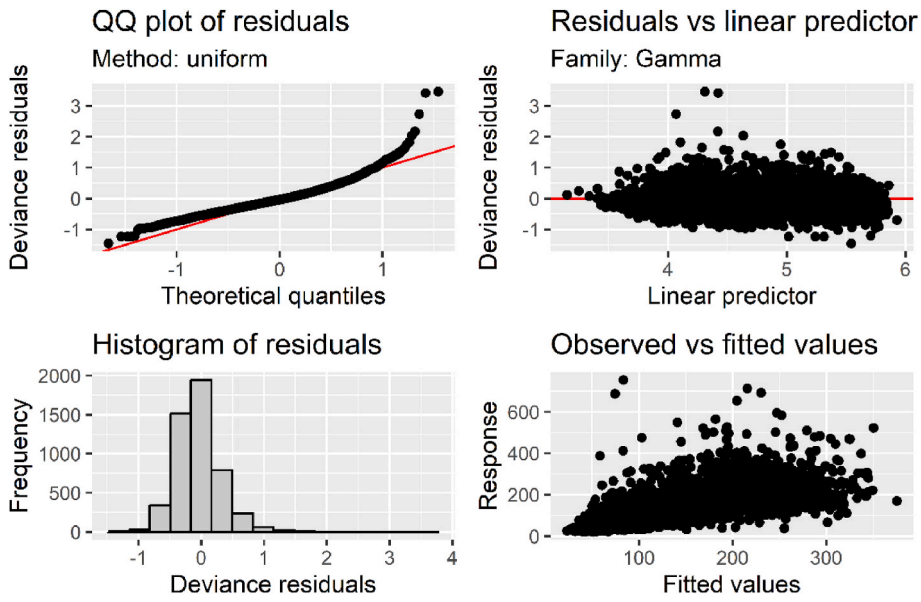

Fig. 8. Model check plots for meteorology-adjusted model for $PM_{2.5}$ at Delhi for 2007–2022.

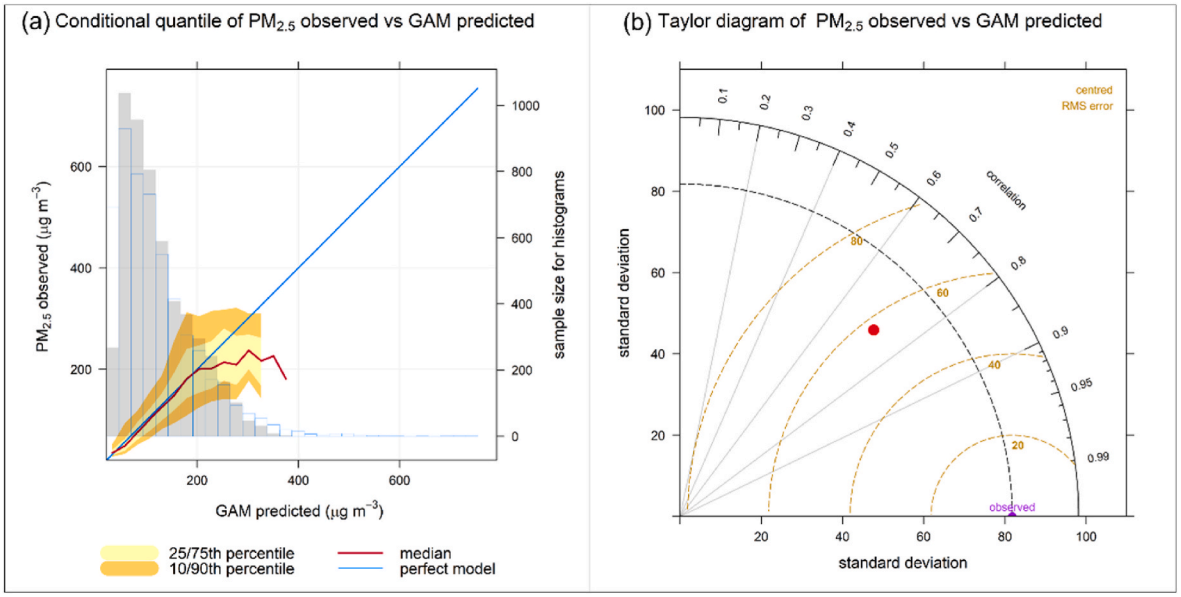

Fig. 9. a) Conditional quantile plot and **b)** Taylor diagram showing the GAM model performance statistics for predicting the $PM_{2.5}$ concentration in Delhi.

percentiles of the GAM predictions. The dark red curve shows the median of the GAM predicted values, while the light blue histogram and straight line depict the observed values. The grey-shaded area represents the histogram of the GAM predicted values. The graph compares the meteorology-adjusted GAM prediction quantiles against the observed concentration quantiles. The median of the model predicted quantiles closely follows the perfect model up to 200 μg m^{-3}. The light-yellow region, which represents the 25/75 percentile of the model predicted quantiles, accommodates the actual concentration quantiles (light blue line) for all values up to approximately 300 μg m^{-3}. However, at higher concentrations, the model underestimates high $PM_{2.5}$ peaks, resulting in significant deviation. The model's performance was also evaluated using the Taylor's diagram shown in Fig. 9b. It shows correlation coefficient, standard deviation and centred RMS error in a 2-D plot. The model underestimates the variability of $PM_{2.5}$ concentration because it lies below the dashed black line. A high correlation coefficient (r = 0.7, shown by a red circle) indicates a close agreement between the observation and model output. The root mean square error in the model is 57 μg m^{-3}.

Here n, FAC2, MB, MGE, NMGE, RMSE, COE, IOA, r represents the number of days used for model evaluation, the fraction of prediction within a factor of two, mean bias, mean gross error, normalised mean gross error, root mean squared error, coefficient of efficiency, index of agreement, and Pearson correlation coefficient between the observed and GAM predicted values. Table 2 shows that GAM performed fairly well for $PM_{2.5}$ during the study period. $PM_{2.5}$ model evaluation results are based on 5327 days.

3.4. GAM as a prediction tool

GAM serves as a prediction tool for estimating $PM_{2.5}$ concentration using solely meteorological and time variables. Firstly, the GAM was trained for the training data set, which here includes the trend estimation period from 2007 to 2022, except for a cross-validation test year,

Table 2
A summary of statistics for the GAM performance for $PM_{2.5}$.

Pollutant	n	FAC2	MB	MGE	NMGE	RMSE	COE	IOA	r
$PM_{2.5}$	5327	0.93	0.09	35.91	0.29	57.16	0.42	0.71	0.72

which is selected here as 2022 (cross-validation results for other years are shown in the Supplement Figs. S7–S11). Fig. 10, displays the $PM_{2.5}$ concentration predictions for 2022, represented by both observed (blue) and meteorology-adjusted GAM predicted (red) values. The observed and GAM-predicted values are in close agreement, except for the episodic high values, which were strongly underestimated by GAM. This may be because most episodic events were associated with the long-range transport.

In Delhi, dust storms occurring in March-April are attributed to long-range transport, specifically Arabian dust, and medium-range transport, from the Thar desert of Rajasthan (Kumar et al., 2014; Sarkar et al., 2019; Singh et al., 2022). In contrast, smoke and precursor gases are transported to Delhi during October-November medium-range transport from Punjab, Haryana, and eastern Uttar Pradesh, intensifying the already elevated $PM_{2.5}$ levels (Jethva et al., 2018; Montes et al., 2022; Takigawa et al., 2020). Unfortunately, the AirGAM model inadequately estimates the effects of long-range transport due to its dependence on local meteorology and time variables alone. Notably, the model relies on the day-of-year parameter to learn about high peaks resulting from stubble-burning emissions in October-November.

Using 16 years of data, the model has established smooth non-linear functions to predict $PM_{2.5}$ concentration levels. However, the model's limited ability to predict peaks is not solely attributed to the stark differences in meteorological conditions between Delhi and neighboring states where stubble is burned. The variability of burning emissions strongly influences it, as fire events do not consistently occur on the same day each year.

It's important to acknowledge that the model's limitation persists because it relies exclusively on meteorological and time covariates to predict $PM_{2.5}$ levels. The model lacks information regarding emissions, background conditions, and the formation of secondary particulates through precursor gases. Despite these limitations, it's noteworthy that the model demonstrates satisfactory performance with minimal input from meteorology and time. Nonetheless, the model demonstrated overall satisfactory performance and can be used to predict $PM_{2.5}$ concentrations using only meteorology and time variables with reasonably good accuracy under more regular conditions, where long-range transport is less important.

3.5. Theil-Sen trends in meteorological parameters

Since meteorology affects the $PM_{2.5}$ concentration, we also calculated the Theil-Sen linear trends for all meteorological parameters during 2007–2022 over Delhi. Fig. 11 shows that except for temperature, statistically significant trends were observed in wind speed, wind direction, relative humidity, planetary boundary layer height, and rainfall. A small but significant rising trend were observed in relative humidity (0.35% $year^{-1}$ with $p < 0.001$) and rainfall (0.03 mm day^{-1} $year^{-1}$ with $p < 0.001$). Wind speed (−0.01 m s^{-1} $year^{-1}$ with $p < 0.05$) and PBLH (−1.76 m $year^{-1}$ with $p < 0.05$) exhibited a declining trend. The 95% confidence interval of the trends are shown in the square bracket on each subplot. Our study demonstrates that the effects of inter-annual variations in meteorology over $PM_{2.5}$ long-term trends were minimal during the study period. GAM unadjusted and meteorology-adjusted $PM_{2.5}$ trends were very close during 2007–2014 and overlapped each other during 2015–2022.

4. Conclusions

The present study examines the trends in $PM_{2.5}$ levels in Delhi from 2007 to 2022, both with and without adjustments for meteorology. The recent AirGAM 2022r1 model was used, considering daily averages of $PM_{2.5}$ and meteorological data. The model estimated the influence of meteorological variability on fine particle pollution trends over the city. The study found that while there were slight downward trends in both unadjusted (14 μg m^{-3}) and meteorology-adjusted (18 μg m^{-3}) $PM_{2.5}$ levels, the impact of meteorological changes on fine particle pollution was minimal. The model had an adj. R^2 of 0.55, with covariates day-of-year and years (associated with the trend) being statistically significant. Day-of-week and medium height cloud cover were insignificant. Wind speed was the most influential factor, followed by planetary boundary layer height and temperature. However, all meteorological parameters had a non-linear relationship with $PM_{2.5}$. The model performed well in predicting $PM_{2.5}$ levels (correlation of 0.7), but underestimated peak levels, which is linked to long-range transport of pollutants. Over time, relative humidity and rainfall have shown increasing trends, while wind speed and planetary boundary layer height exhibited declining trends over Delhi. As for temperature, no significant long-term trends have been observed. Our study demonstrates that the effects of inter-annual variations in meteorology over $PM_{2.5}$ long-term trends were minimal

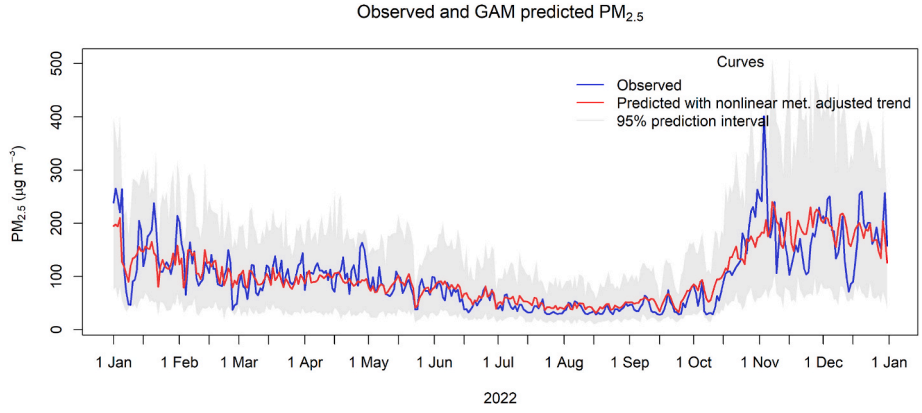

Fig. 10. Observed (blue) and meteorology adjusted GAM predicted (red) concentrations of $PM_{2.5}$ for 2022. The grey-shaded region demonstrates a 95% prediction interval. (For interpretation of the references to colour in this figure legend, the reader is referred to the Web version of this article.)

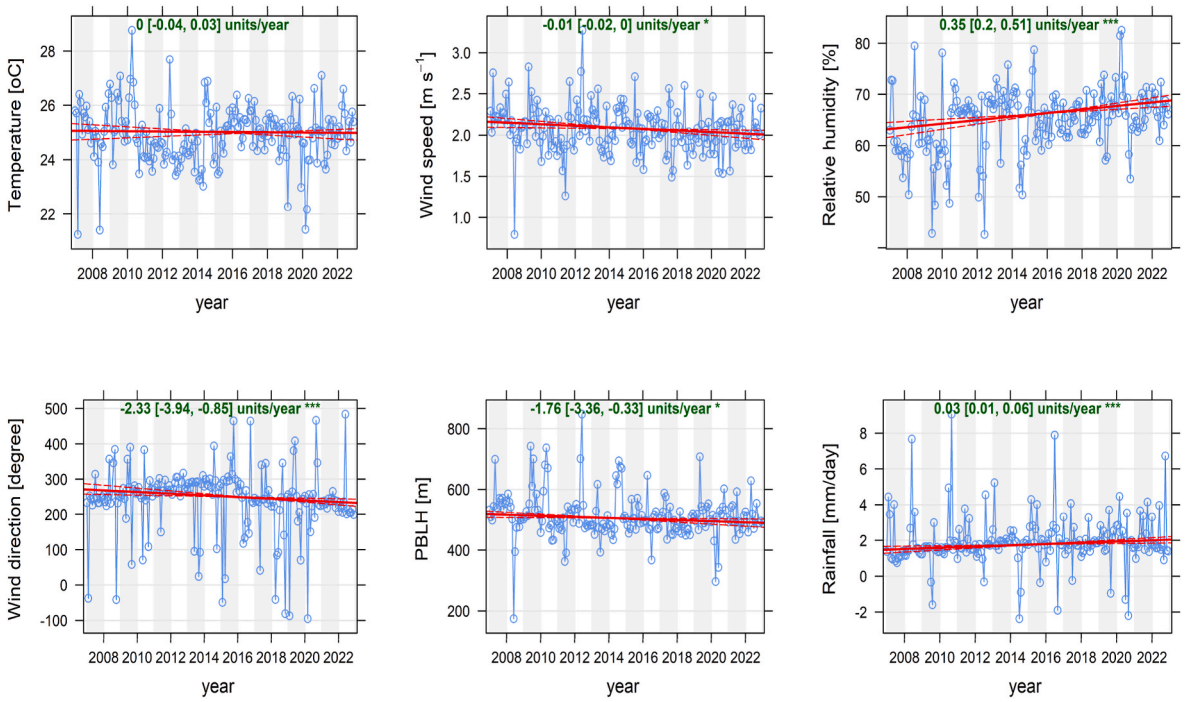

Fig. 11. Theil-Sen linear trends in meteorological parameters including temperature, wind speed, relative humidity, wind direction, planetary boundary layer height and rainfall during 2007–2022 over Delhi.

during the study period. The analysis revealed two significant break-points in the $PM_{2.5}$ time series. The first break-point occurred on October 1, 2010, and coincided with a substantial 57% increase in $PM_{2.5}$ levels. This rise is likely attributable to the long-range transport of pollutants. While there have been some improvements in particle pollution, further actions are needed to significantly reduce $PM_{2.5}$ levels through regional joint prevention and control efforts.

CRediT authorship contribution statement

Chetna: Conceptualization, Data curation, Formal analysis, Investigation, Methodology, Software, Visualization, Writing – original draft. **Surendra K. Dhaka:** Supervision, Writing – review & editing. **Sam-Erik Walker:** Conceptualization, Formal analysis, Methodology, Resources, Software, Supervision, Writing – review & editing. **Vikas Rawat:** Data curation, Formal analysis, Resources, Software, Visualization, Writing – review & editing. **Narendra Singh:** Supervision, Writing – review & editing.

Declaration of competing interest

The authors declare that they have no known competing financial interests or personal relationships that could have appeared to influence the work reported in this paper.

Data availability

Data will be made available on request.

Acknowledgments

We would like to acknowledge the significant contribution of Karl Ropkins from Institute for Transport Studies, University of Leeds, Leeds, UK for his insightful feedback and constructive suggestions that have greatly enhanced the quality of this work. This study was supported by the Research Institute for Humanity and Nature, Japan (RIHN: a constituent member of NIHU), Project no 14200133. Authors are thankful to Prof. Sachiko Hayashida, Prof. Yutaka Matsumi, and Prof. Prabir Patra, and Dr. Vinay Kumar for their suggestions and advice for properly carrying out this piece of work. The Authors also thank European Centre for Medium-Range Weather Forecasts for making the ERA5 data set available through the Copernicus Climate Change Service. The use of the Central Pollution Control Board (CPCB), Delhi Pollution Control Committee (DPCC), Indian Meteorological Department (IMD), and U.S. Embassy and Consulates in New Delhi for providing surface data of $PM_{2.5}$ online is gratefully acknowledged.

Appendix A. Supplementary data

Supplementary data to this article can be found online at https://doi.org/10.1016/j.aeaoa.2024.100255.

References

Carslaw, D.C., Ropkins, K., 2012. openair—an R package for air quality data analysis. Environ. Model. Software 27–28, 52–61. https://doi.org/10.1016/j.envsoft.2011.09.008.

Central Pollution Control Board (CPCB), 2009. National ambient air quality standards. Central Pollution Control Board. https://cpcb.nic.in/displaypdf.php?id=aG9tZS9haXItcG9sbHV0aW9uL1JlY3ZlZC1OYXRpb25hbC5wZGY=.

Central Pollution Control Board (CPCB), 2012. Central Pollution Control Board (2012-2013). Guidelines for the measurements of the ambient air pollutants. P R Division, CPCB 1 iii. 83.

Chetna, Dhaka S.K., Longiany, G., Panwar, V., Kumar, V., Malik, S., Singh, N., Dimri, A. P., Matsumi, Y., Nakayama, T., Hayashida, S., 2022. Trends and variability of PM2.5 at different time scales over Delhi: long-term analysis 2007-2021. Aerosol Air Qual. Res. 22, 220191 https://doi.org/10.4209/aaqr.220191.

Dhaka, S.K., Chetna, Kumar, V., Panwar, V., Dimri, A.P., Singh, N., Patra, P.K., Matsumi, Y., Takigawa, M., Nakayama, T., Yamaji, K., Kajino, M., Misra, P., Hayashida, S., 2020. PM2.5 diminution and haze events over Delhi during the COVID-19 lockdown period: an interplay between the baseline pollution and meteorology. Sci. Rep. 10 (1) https://doi.org/10.1038/s41598-020-70179-8. Article 1.

Enayati Ahangar, F., Pakbin, P., Hasheminassab, S., Epstein, S.A., Li, X., Polidori, A., Low, J., 2021. Long-term trends of PM2.5 and its carbon content in the South Coast Air Basin: a focus on the impact of wildfires. Atmos. Environ. 255, 118431 https://doi.org/10.1016/j.atmosenv.2021.118431.

Fu, X., Wang, X., Hu, Q., Li, G., Ding, X., Zhang, Y., He, Q., Liu, T., Zhang, Z., Yu, Q., Shen, R., Bi, X., 2016. Changes in visibility with PM2.5 composition and relative

humidity at a background site in the Pearl River Delta region. J. Environ. Sci. 40, 10–19. https://doi.org/10.1016/j.jes.2015.12.001.
Fuzzi, S., Baltensperger, U., Carslaw, K., Decesari, S., Denier van der Gon, H., Facchini, M.C., Fowler, D., Koren, I., Langford, B., Lohmann, U., Nemitz, E., Pandis, S., Riipinen, I., Rudich, Y., Schaap, M., Slowik, J.G., Spracklen, D.V., Vignati, E., Wild, M., et al., 2015. Particulate matter, air quality and climate: lessons learned and future needs. Atmos. Chem. Phys. 15 (14), 8217–8299. https://doi.org/10.5194/acp-15-8217-2015.
Gao, Z., Ivey, C.E., Blanchard, C.L., Do, K., Lee, S.-M., Russell, A.G., 2023. Emissions, meteorological and climate impacts on PM2.5 levels in Southern California using a generalized additive model: historic trends and future estimates. Chemosphere 325, 138385. https://doi.org/10.1016/j.chemosphere.2023.138385.
Geiß, A., Wiegner, M., Bonn, B., Schäfer, K., Forkel, R., von Schneidemesser, E., Münkel, C., Chan, K.L., Nothard, R., 2017. Mixing layer height as an indicator for urban air quality? Atmos. Meas. Tech. 10 (8), 2969–2988. https://doi.org/10.5194/amt-10-2969-2017.
Grange, S.K., Carslaw, D.C., 2019. Using meteorological normalisation to detect interventions in air quality time series. Sci. Total Environ. 653, 578–588. https://doi.org/10.1016/j.scitotenv.2018.10.344.
Grange, S.K., Carslaw, D.C., Lewis, A.C., Boleti, E., Hueglin, C., 2018. Random forest meteorological normalisation models for Swiss PM10 trend analysis. Atmos. Chem. Phys. 18 (9), 6223–6239. https://doi.org/10.5194/acp-18-6223-2018.
Hammer, M.S., van Donkelaar, A., Li, C., Lyapustin, A., Sayer, A.M., Hsu, N.C., Levy, R. C., Garay, M.J., Kalashnikova, O.V., Kahn, R.A., Brauer, M., Apte, J.S., Henze, D.K., Zhang, L., Zhang, Q., Ford, B., Pierce, J.R., Martin, R.V., 2020. Global estimates and long-term trends of fine particulate matter concentrations (1998–2018). Environ. Sci. Technol. 54 (13), 7879–7890. https://doi.org/10.1021/acs.est.0c01764.
Hastie, T.J., Tibshirani, R.J., 2017. Generalized Additive Models, first ed. Routledge. https://doi.org/10.1201/9780203753781.
Hastie, T., Tibshirani, R., 1990. Generalized Additive Models. Chapman and Hall, London and New York.
Hersbach, H., Bell, B., Berrisford, P., Hirahara, S., Horányi, A., Muñoz-Sabater, J., Nicolas, J., Peubey, C., Radu, R., Schepers, D., Simmons, A., Soci, C., Abdalla, S., Abellan, X., Balsamo, G., Bechtold, P., Biavati, G., Bidlot, J., Bonavita, M., et al., 2020. The ERA5 global reanalysis. Q. J. R. Meteorol. Soc. 146 (730), 1999–2049. https://doi.org/10.1002/qj.3803.
Indian Meteorological Department (IMD), 2015. Glossary. Indian Meteorological Department. https://www.imdpune.gov.in/Weather/Reports/glossary.pdf.
Ito, K., Thurston, G.D., Silverman, R.A., 2007. Characterization of PM2.5, gaseous pollutants, and meteorological interactions in the context of time-series health effects models. J. Expo. Sci. Environ. Epidemiol. 17 (S2), S45–S60. https://doi.org/10.1038/sj.jes.7500627.
Jain, S., Sharma, S.K., Srivastava, M.K., Chatterjee, A., Vijayan, N., Tripathy, S.S., Kumari, K.M., Mandal, T.K., Sharma, C., 2021. Chemical characterization, source apportionment and transport pathways of PM2.5 and PM10 over Indo Gangetic Plain of India. Urban Clim. 36, 100805 https://doi.org/10.1016/j.uclim.2021.100805.
Jain, S., Sharma, S.K., Vijayan, N., Mandal, T.K., 2020. Seasonal characteristics of aerosols (PM2.5 and PM10) and their source apportionment using PMF: a four year study over Delhi, India. Environ. Pollut. 262, 114337 https://doi.org/10.1016/j.envpol.2020.114337.
Jethva, H., Chand, D., Torres, O., Gupta, P., Lyapustin, A., Patadia, F., 2018. Agricultural burning and air quality over northern India: a synergistic analysis using NASA's A-train satellite data and ground measurements. Aerosol Air Qual. Res. 18.
Jing, Z., Liu, P., Wang, T., Song, H., Lee, J., Xu, T., Xing, Y., 2020. Effects of meteorological factors and anthropogenic precursors on PM2.5 concentrations in cities in China. Sustainability 12 (9), 3550. https://doi.org/10.3390/su12093550.
Kendall, M.G., 1975. Rank Correlation Methods, fourth ed. Charles Griffin, London.
Kumar, R., Barth, M.C., Pfister, G.G., Naja, M., Brasseur, G.P., 2014. WRF-Chem simulations of a typical pre-monsoon dust storm in northern India: influences on aerosol optical properties and radiation budget. Atmos. Chem. Phys. 16.
Latha, R., Mukherjee, A., Dahiya, K., Bano, S., Pawar, P., Kalbande, R., Maji, S., Beig, G., Murthy, B.S., 2022. On the varied emission fingerprints of particulate matter over typical locations of NCR (Delhi) – a perspective for mitigation plans. J. Environ. Manag. 311, 114834 https://doi.org/10.1016/j.jenvman.2022.114834.
Li, L., Qian, J., Ou, C.-Q., Zhou, Y.-X., Guo, C., Guo, Y., 2014. Spatial and temporal analysis of Air Pollution Index and its timescale-dependent relationship with meteorological factors in Guangzhou, China, 2001–2011. Environ. Pollut. 190, 75–81. https://doi.org/10.1016/j.envpol.2014.03.020.
Liao, H., Chang, W., Yang, Y., 2015. Climatic effects of air pollutants over China: a review. Adv. Atmos. Sci. 32 (1), 115–139. https://doi.org/10.1007/s00376-014-0013-x.
Lin, X., Liao, Y., Hao, Y., 2018. The burden associated with ambient PM2.5 and meteorological factors in Guangzhou, China, 2012–2016: a generalized additive modeling of temporal years of life lost. Chemosphere 212, 705–714. https://doi.org/10.1016/j.chemosphere.2018.08.129.
Lu, X., Zhang, L., Shen, L., 2019. Meteorology and climate influences on tropospheric ozone: a review of natural sources, chemistry, and transport patterns. Curr. Pollut. Rep. 5 (4), 238–260. https://doi.org/10.1007/s40726-019-00118-3.
Luan, T., Guo, X., Guo, L., Zhang, T., 2018. Quantifying the relationship between $PM_{2.5}$ concentration, visibility and planetary boundary layer height for long-lasting haze and fog–haze mixed events in Beijing. Atmos. Chem. Phys. 18 (1), 203–225. https://doi.org/10.5194/acp-18-203-2018.
Ma, Y., Yang, S., Zhou, J., Yu, Z., Zhou, J., 2018. Effect of ambient air pollution on emergency room admissions for respiratory diseases in Beijing, China. Atmos. Environ. 191, 320–327. https://doi.org/10.1016/j.atmosenv.2018.08.027.
Mann, H.B., 1945. Nonparametric tests against trend. Econometrica 13 (3), 245. https://doi.org/10.2307/1907187.
MetOne, M., 2020. BAM 1022 particulate monitor operation manual. https://metone.com/wp-content/uploads/2020/02/BAM-1022-9805-Operation-Manual-Rev-C.pdf.
Miao, Y., Liu, S., Guo, J., Huang, S., Yan, Y., Lou, M., 2018. Unraveling the relationships between boundary layer height and PM2.5 pollution in China based on four-year radiosonde measurements. Environ. Pollut. 243, 1186–1195. https://doi.org/10.1016/j.envpol.2018.09.070.
Montes, C., Sapkota, T., Singh, B., 2022. Seasonal patterns in rice and wheat residue burning and surface PM2.5 concentration in northern India. Atmos. Environ. X 13, 100154. https://doi.org/10.1016/j.aeaoa.2022.100154.
Muggeo, V.M., 2008. Segmented: an R package to fit regression models with broken-line relationships. R. News 8 (1), 20–25.
Muggeo, V.M.R., 2003. Estimating regression models with unknown break-points. Stat. Med. 22 (19), 3055–3071. https://doi.org/10.1002/sim.1545.
Muggeo, V.M.R., 2017. Interval estimation for the breakpoint in segmented regression: a smoothed score-based approach. Aust. N. Z. J. Stat. 59 (3), 311–322. https://doi.org/10.1111/anzs.12200.
Muggeo, V.M.R., 2023. Segmented: Regression Models with Break-Points/Change-Points (With Possibly Random Effects) Estimation, 1.vols. 6–4 [Computer software]. https://cran.r-project.org/web/packages/segmented/index.html.
Nagpure, A.S., Ramaswami, A., Russell, A., 2015. Characterizing the spatial and temporal patterns of open burning of municipal solid waste (MSW) in Indian cities. Environ. Sci. Technol. 49 (21), 12904–12912. https://doi.org/10.1021/acs.est.5b03243.
Pearce, J.L., Beringer, J., Nicholls, N., Hyndman, R.J., Tapper, N.J., 2011. Quantifying the influence of local meteorology on air quality using generalized additive models. Atmos. Environ. 45 (6), 1328–1336. https://doi.org/10.1016/j.atmosenv.2010.11.051.
R Core Team, 2022. R: A Language and Environment for Statistical Computing. R Foundation for Statistical Computing, Vienna, Austria. https://www.r-project.org/.
Rawat, V., Singh, N., Singh, J., Rajput, A., Dhaka, S.K., Matsumi, Y., Nakayama, T., Hayashida, S., 2023. Assessing the high-resolution PM2.5 measurements over a Central Himalayan site: impact of mountain meteorology and episodic events. Air Qual. Atmosph. Health. https://doi.org/10.1007/s11869-023-01429-7.
Ropkins, K., Carslaw, D.C., 2012. Openair—data analysis tools for the air quality community. The R Journal 4 (1), 20. https://doi.org/10.32614/RJ-2012-003.
Ropkins, K., Tate, J.E., 2021. Early observations on the impact of the COVID-19 lockdown on air quality trends across the UK. Sci. Total Environ. 754, 142374 https://doi.org/10.1016/j.scitotenv.2020.142374.
Ropkins, K., Tate, J.E., Walker, A., Clark, T., 2022. Measuring the impact of air quality related interventions. Environ. Sci.: Atmospheres 2 (3), 500–516. https://doi.org/10.1039/D1EA00073J.
Ropkins, K., Walker, A., Tate, J., 2023. AQEval: air quality evaluation [Computer software], 0.5.2. https://cran.r-project.org/web/packages/AQEval/index.html.
Sarkar, S., Chauhan, A., Kumar, R., Singh, R.P., 2019. Impact of deadly dust storms (may 2018) on air quality, meteorological, and atmospheric parameters over the northern parts of India. GeoHealth 3 (3), 67–80. https://doi.org/10.1029/2018GH000170.
Sen, P.K., 1968. Estimates of regression coefficient based on Kendall's tau. J. Am. Stat. Assoc. 63 (324), 1379–1389.
Sharma, D., Mauzerall, D., 2022. Analysis of air pollution data in India between 2015 and 2019. Aerosol Air Qual. Res. 22 (2), 210204 https://doi.org/10.4209/aaqr.210204.
Sharma, S.K., Mandal, T.K., Banoo, R., Rai, A., Rani, M., 2022. Long-term variation in carbonaceous components of PM2.5 from 2012 to 2021 in Delhi. Bull. Environ. Contam. Toxicol. https://doi.org/10.1007/s00128-022-03506-6.
Sharma, S.K., Mandal, T.K., Sharma, A., Saraswati, Jain, S., 2018. Seasonal and annual trends of carbonaceous species of PM10 over a megacity Delhi, India during 2010–2017. J. Atmos. Chem. 75 (3), 305–318. https://doi.org/10.1007/s10874-018-9379-y.
Singh, J., Singh, N., Ojha, N., Srivastava, A.K., Bisht, D.S., Rajeev, K., Kumar, K.N.V.P., Singh, R.S., Panwar, V., Dhaka, S.K., Kumar, V., Nakayama, T., Matsumi, Y., Hayashida, S., Dimri, A.P., 2022. Genesis of a severe dust storm over the Indian subcontinent: dynamics and impacts. Earth Space Sci. 9 (2), e2021EA001702 https://doi.org/10.1029/2021EA001702.
Singh, T., Saha, U., Prasad, V.S., Gupta, M.D., 2021. Assessment of newly-developed high resolution reanalyses (IMDAA, NGFS and ERA5) against rainfall observations for Indian region. Atmos. Res. 259, 105679 https://doi.org/10.1016/j.atmosres.2021.105679.
Singh, V., Singh, S., Biswal, A., 2021. Exceedances and trends of particulate matter (PM2.5) in five Indian megacities. Sci. Total Environ. 750, 141461 https://doi.org/10.1016/j.scitotenv.2020.141461.
Solberg, S., Colette, A., Raux, B., Walker, S.-E., Guerreiro, C., 2021. Long-term trends of air pollutants at national level 2005-2019. ETC/ATNI Eionet Report 9/2021, European Topic Centre on Air Pollution and Climate Change Mitigation. https://www.eionet.europa.eu/etcs/etc-atni/products/etc-atni-reports/etc-atni-report-9-2021-long-term-trends-of-air-pollutants-at-national-level-2005-2019.
Solberg, S., Walker, S.-E., Schneider, P., Guerreiro, C., 2021b. Quantifying the impact of the covid-19 lockdown measures on nitrogen dioxide levels throughout Europe. Atmosphere 12 (2), 131. https://doi.org/10.3390/atmos12020131.
Stiglic, G., Kocbek, P., Fijacko, N., Zitnik, M., Verbert, K., Cilar, L., 2020. Interpretability of machine learning-based prediction models in healthcare. WIREs Data Mining and Knowledge Discovery 10 (5), e1379. https://doi.org/10.1002/widm.1379.
Su, T., Li, Z., Kahn, R., 2018. Relationships between the planetary boundary layer height and surface pollutants derived from lidar observations over China: regional pattern and influencing factors. Atmos. Chem. Phys. 18 (21), 15921–15935. https://doi.org/10.5194/acp-18-15921-2018.

Takigawa, M., Patra, P.K., Matsumi, Y., Dhaka, S.K., Nakayama, T., Yamaji, K., Kajino, M., Hayashida, S., 2020. Can Delhi's Pollution Be Affected by Crop Fires in the Punjab Region?, vol. 16, p. 6.

Tella, A., Balogun, A.-L., Faye, I., 2021. Spatio-temporal modelling of the influence of climatic variables and seasonal variation on PM 10 in Malaysia using multivariate regression (MVR) and GIS. Geomatics, Nat. Hazards Risk 12 (1), 443–468. https://doi.org/10.1080/19475705.2021.1879942.

The Automotive Research Association of India and The Energy and Resources Institute (ARAI and TERI), 2018. Source apportionment of PM2.5 & PM10 of Delhi NCR for identification of major sources. Report No. ARAI/16-17/DHI-SA-NCR/Final Report, Department of Heavy Industry Ministry of Heavy Industries and Public Enterprises, New Delhi, India. https://www.teriin.org/sites/default/files/2018-08/Report_SA_AQM-Delhi-NCR_0.pdf.

Theil, H., 1950. A rank invariant method of linear and polynomial regression analysis, I, II, III. Proc. Koninklijke Nederlandse Akademie Wetenschappen, Series A – Math. Sci. 53, 386–392, 521–25, 1397–392.

U.S. Environmental Protection Agency (U.S. EPA), 2023. List of designated reference and equivalent methods. https://www.epa.gov/system/files/documents/2023-06/List_of_FRM_FEM_%20June%202023_Final.pdf. (Accessed 15 June 2022).

Vishal, J.K., Rani, S.I., 2022. Location-specific verification of near-surface air temperature from IMDAA regional reanalysis. J. Earth Syst. Sci. 131 (3), 179. https://doi.org/10.1007/s12040-022-01935-9.

Walker, S.-E., Solberg, S., Schneider, P., Guerreiro, C., 2023. The AirGAM 2022r1 air quality trend and prediction model. Geosci. Model Dev. (GMD) 16, 573–595. https://doi.org/10.5194/gmd-16-573-2023, 2023.

Wang, J., Ogawa, S., 2015. Effects of meteorological conditions on PM2.5 concentrations in nagasaki, Japan. Int. J. Environ. Res. Publ. Health 12 (8), 9089–9101. https://doi.org/10.3390/ijerph120809089.

Whiteman, C.D., Hoch, S.W., Horel, J.D., Charland, A., 2014. Relationship between particulate air pollution and meteorological variables in Utah's Salt Lake Valley. Atmos. Environ. 94, 742–753. https://doi.org/10.1016/j.atmosenv.2014.06.012.

Wood, S., 2023. Mgcv: Mixed GAM Computation Vehicle with Automatic Smoothness Estimation, 1.vols. 9–0 [Computer software]. https://cran.r-project.org/web/packages/mgcv/index.html.

Wood, S.N., 2017. Generalized Additive Models: an Introduction with R, second ed. Chapman and Hall/CRC. https://doi.org/10.1201/9781315370279.

Worldatlas, 2018. Cities with the worst air quality in Asia. https://www.worldatlas.com/articles/cities-with-the-worst-air-quality-in-asia.html.

Wu, Z., Zhang, S., 2019. Study on the spatial–temporal change characteristics and influence factors of fog and haze pollution based on GAM. Neural Comput. Appl. 31 (5), 1619–1631. https://doi.org/10.1007/s00521-018-3532-z.

Yang, X., Jiang, L., Zhao, W., Xiong, Q., Zhao, W., Yan, X., 2018. Comparison of ground-based PM2.5 and PM10 concentrations in China, India, and the U.S. Int. J. Environ. Res. Publ. Health 15 (7), 1382. https://doi.org/10.3390/ijerph15071382.

Yang, X., Zhao, C., Guo, J., Wang, Y., 2016. Intensification of aerosol pollution associated with its feedback with surface solar radiation and winds in Beijing. J. Geophys. Res. Atmos. 121 (8), 4093–4099. https://doi.org/10.1002/2015JD024645.

Zeileis, A., 2022. Sandwich: robust covariance matrix estimators. https://cran.r-project.org/package=sandwich.

Zeileis, A., Kleiber, C., Jackman, S., 2008. Regression models for count data in R. J. Stat. Software 27 (8). https://doi.org/10.18637/jss.v027.i08.

Zeileis, A., Kleiber, C., Krämer, W., Hornik, K., 2003. Testing and dating of structural changes in practice. Comput. Stat. Data Anal. 44 (1–2), 109–123. https://doi.org/10.1016/S0167-9473(03)00030-6.

Zeileis, A., Leisch, F., Hornik, K., Kleiber, C., 2002. Strucchange: an R package for testing for structural change in linear regression models. J. Stat. Software 7, 1–38. https://doi.org/10.18637/jss.v007.i02.

Zhang, R., Wang, G., Guo, S., Zamora, M.L., Ying, Q., Lin, Y., Wang, W., Hu, M., Wang, Y., 2015. Formation of urban fine particulate matter. Chem. Rev. 115 (10), 3803–3855. https://doi.org/10.1021/acs.chemrev.5b00067.